High Performance Sputtered PZT Film for MEMS Applications

Y. Hishinuma[*1], Y. Li[*] and J. Birkmeyer[*]
T. Fujii[**2],T. Naono[**] and T. Arakawa[**]

[*]FUJIFILM Dimatix, Inc., 2250 Martin Avenue, Santa Clara, California, 95050, USA
[1]yhishinuma@fujifilm.com
[**]FUJIFILM Corp., 577 Ushijima, Kaisei-machi, Ashigarakami-gun, Kanagawa-ken, Japan
[2]takamichi_fujii@fujifilm.co.jp

ABSTRACT

We have developed a method of forming PZT films on silicon substrates with a high piezoelectric coefficient using RF sputtering. Films have been formed on 6 inch wafers with thickness variation of less than +/-5% across the entire wafer. Our PZT film has an unusually high content of Nb dopant (13%) which results in ×1.7 higher piezoelectric coefficient than sputtered PZT films previously reported. The x-ray diffraction patterns of our PZT film formed on a 6 inch wafer demonstrate that film is in a perovskite phase with (100) orientation which partly accounts for its high piezoelectric performance. One of the unique properties of our sputtered PZT film can be observed in the hysteresis loop shifted to the positive electric field, suggesting that the polarization axes have been aligned in a certain direction beforehand, making a post-deposition polarization process unnecessary. A displacement measurement using a diaphragm structure yielded d_{31}= -250pm/V. Additionally, 4-point cantilever bending experiment yielded $e_{31,f}$= -23.1 C/m^2.

Keywords: PZT, MEMS, piezoelectric coefficients, $e_{31,f}$, d_{31}

1 INTRODUCTION

Lead zirconate titanate (PZT) films have been used for ferroelectric random access memory (FeRAM) as well as sensors and actuators by combining them with MEMS technologies [1]. Methods for PZT film deposition include sol-gel, sputtering, aerosol deposition, and CVD with each of them having its own advantages and disadvantages [2-9].

In previous work, the authors have successfully formed and characterized PZT and Nb-doped PZT (PNZT) films deposited on silicon wafers by sputtering, and have demonstrated that PNZT has much superior piezoelectric characteristics compared to non-doped PZT [10, 11]. Since then, the work has been extended to a high volume production level on 6-inch wafer tool. In this paper, characterization results of PNZT films formed by the production tool and its uniformity across a wafer are presented.

2 SPUTTERED PZT FILM FORMATION AND EVALUATION METHODS

PNZT films were formed by RF-magnetron sputtering. Bottom electrode consisting of TiW 20nm as an adhesion layer followed by Ir 300nm was formed on silicon wafer by sputtering. A sintered PNZT target with Zr to Ti content set to MPB ratio was used. Additionally, 13% Nb was added in order to improve the piezoelectric properties of sputtered film. Films were formed to 1~6μm thickness with a deposition rate of 4μm/hr. Fig.1 shows a photograph of 3μm thick PNZT film deposited on a 6” wafer. A series of characterizations were conducted on the obtained films including XRD for crystal structure, cross-section SEM and TEM for film morphology, P-E hysteresis loops and dielectric constant. In order to characterize piezoelectric properties, diaphragm structures were fabricated using SOI wafer, as well as cantilever structures on a standard silicon wafer.

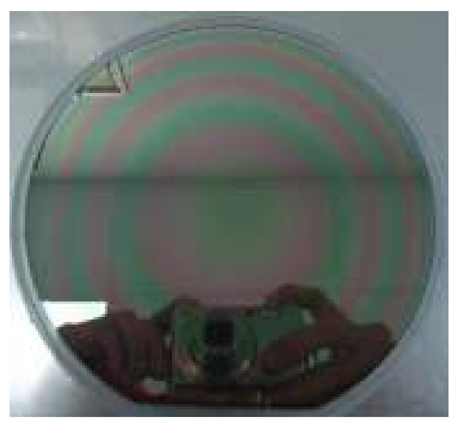

Figure 1: 3μm thick sputtered Nb-PZT film on 6” wafer.

3 CRYSTAL STRUCTURE OF FILMS

Fig 2 shows typical XRD patterns of the PNZT film obtained at five locations on a 6” wafer. Strong diffraction peaks were observed at 21.9º and 44.6º with neglible peaks from other phases. Uniformity of the diffraction pattern across the wafer is also very good. Uniaxial orientation in perovskite (100) phase ensures that the obtained film generates the maximum converse piezoelectric effect it can provide.

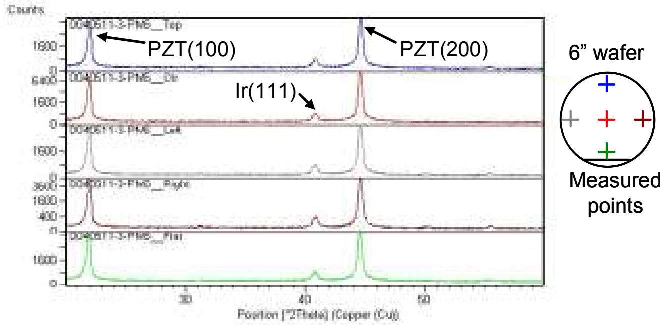

Figure 2: X-ray diffraction patterns of sputtered PNZT film at 5 locations on 6” wafer

Compositional analysis was conducted on obtained film by XRF. Table 1 shows the result at five locations on a wafer. 13% of Nb was incorporated into the film which partly accounts for high piezoelectricity of the film. This is unusually high content of Nb in PZT, as Nb of 3 at.% or more causes pyrochlore phase formation [12] and cracks in film if deposited with normal conditions.

	Pb/(Zr+Ti+Nb)	Zr/(Zr+Ti)	Ti/(Zr+Ti)	Nb/(Zr+Ti+Nb)
Top	1.095	0.505	0.495	0.130
Left	1.099	0.505	0.495	0.130
Center	1.121	0.506	0.494	0.128
Right	1.085	0.503	0.497	0.130
Flat	1.086	0.502	0.498	0.129

Table 1: Composition of sputtered PNZT film on 6” wafer.

Fig. 3 is an SEM micrograph of PNZT film cross-section, showing densely packed columnar structures with very a smooth top surface. A cross-sectional TEM image of the film is shown in Fig.4. No deposits or voids were observed at grain boundaries or at bottom electrode interface.

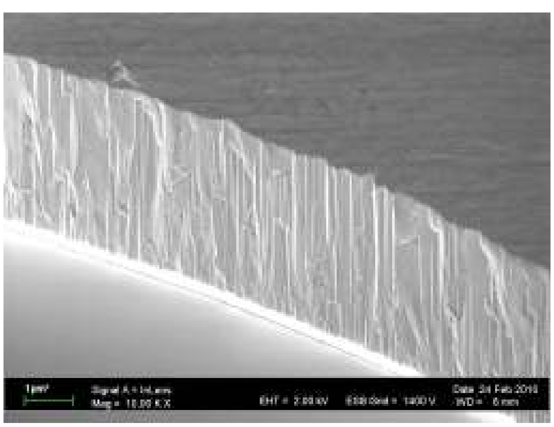

Figure 3: SEM micrograph of PNZT film cross-section

Figure 4: TEM micrograph of PNZT film cross-section

4 ELECTRIC PROPERTIES

Fig.5 shows polarization versus electric field (P-E) hysteresis loops of the films measured with 400µm diameter top electrodes at 5 locations on a wafer, demonstrating very uniform piezoelectric characteristics across a wafer. The P-E loops are shifted toward higher electric field, suggesting that the polarization axes have been aligned in a certain direction beforehand. This unique feature of the film makes a post-deposition polarization process unnecessary.

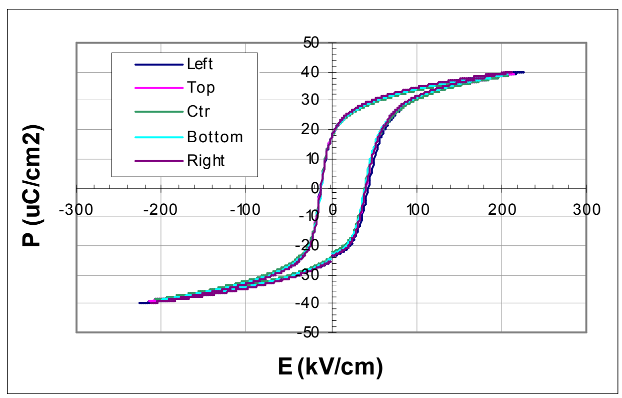

Figure 5: Polarization-Electric field hysteresis loops of sputtered PNZT film at 5 locations on 6” wafer

The dielectric constant of the film measured at 1kHz, 1V was ~1200, which is relatively low considering high piezoelectric coeffcient of the film. Table 2 shows typical measurement results on 3µm thick PNZT film at 5 locations on a wafer showing a good uniformity of electric properties.

	Thickness(μm)	Dielectric Constant	Loss tangent	Pmax(C/m2)
Top	3.01	1161	0.020	38.8
Left	2.98	1139	0.020	38.9
Center	3.14	1209	0.022	37.6
Right	2.99	1136	0.020	39.4
Flat	3.09	1184	0.020	38.9

Table 2: Film thickness, dielectric constant, tanδ and max. polarization of PNZT film at 5 locations on a wafer.

5 PIEZOELECTRIC PROPERTIES

In order to characterize mechanical properties of PNZT film, diaphragm structure was fabricated using silicon wafer as shown in Fig. 6. The diaphragm structure was fabricated by bonding SOI wafer onto another silicon wafer which had already etched cavities. Then, the handle silicon of SOI wafer was removed by grinding and etching. This method of diaphragm fabrication ensures accurate cavity dimension which is critical for this measurement. After removing silicon dioxide, bottom electrode and PNZT film were sequentially deposited onto silicon diaphragm. Finally, top electrode was deposited and patterned.

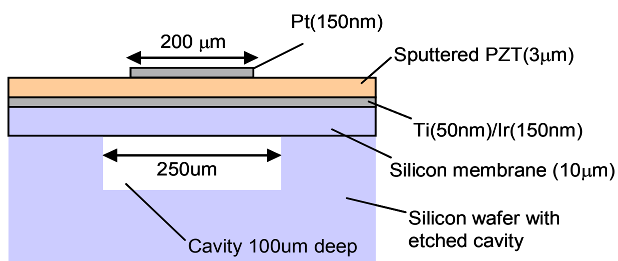

Figure 6: Schematic of diaphragm structure for displacement measurement

From the resonant frequency measurement of the diaphragm and comparison with finite element analysis modeling using ANSYS, the Young's modulus of PNZT film was determined to be 50GPa. In order to activate the diaphragm, a sinusoidal waveform at 10kHz with negative voltage was applied to top electrode while bottom electrode was held at ground. The displacement measurement was taken with a laser Doppler vibrometer. By adjusting the piezoelectric coefficient d_{31} of film in the finite element modeling to match its displacement to measured value, we obtained d_{31}=-250pm/V for our film.

In a separate experiment, the effective transverse piezoelectric coefficient $e_{31,f}$ measurement was conducted using 4-point cantilever bending setup [13]. The $e_{31,f}$ coefficient is considered to be the figure of merit for the majority of MEMS piezoelectric sensors as well as actuators. In this measurement, 3mm × 25mm cantilever is bent with known force so that homogeneous well defined strain profile is generated. The electrical charge generated is measured as a function of strain which gives us $e_{31,f}$. The measurement was conducted by aixACCT Systems GmbH, Germany, and yielded $e_{31,f}$ = -22.1C/m^2 at wafer center and -23.1C/m^2 at wafer edge. As far as authors are aware, this is the highest $e_{31,f}$ achieved for PZT thin film to date.

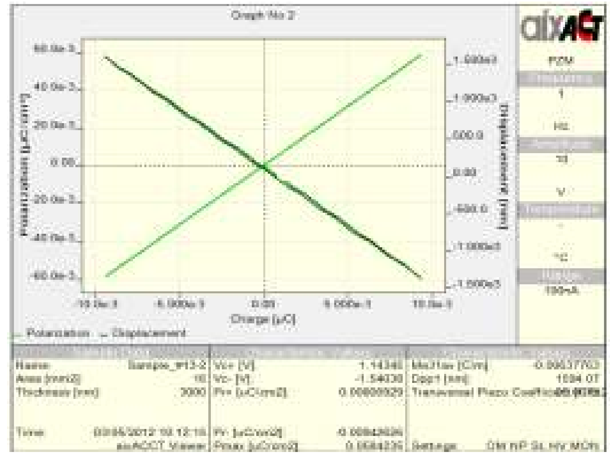

Figure 7: $e_{31,f}$ measurement by aixACCT's 4-point bending setup

6 OTHER FILM PROPERTIES FROM MANUFACTURING STANDPOINT

The sputtered PNZT films also possess extremely high dielectric strength. For 3μm thick film, typical breakdown voltages were over 300V as shown in *I-V* measurement in Fig. 8. For film thickness less 3μm, we constantly obtain dielectric strength over 1MV/cm. As it is known that long-term durability has a strong correlation with dielectric strength, this ensures a good device life time.

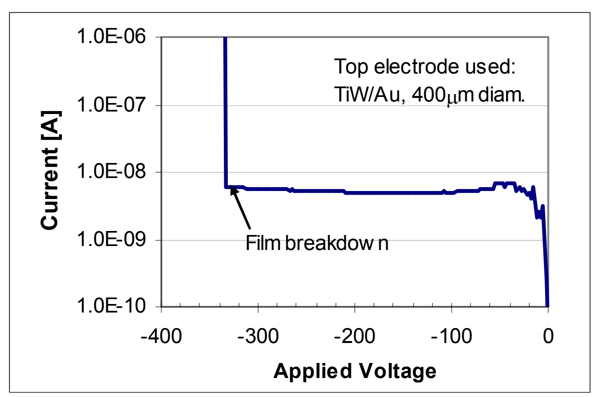

Figure 8: *I-V* measurement on 3μm thick PNZT film.

Another unique feature of the sputtered PNZT film is its resistance to high temperature as described in the following experiment (Fig. 9). In this experiment, the diaphragm sample previously described (Fig.6) was subject to high temperature steps and at each step, displacement was measured at room temperature. The sample was heated up to 500°C without any degradation in displacement.

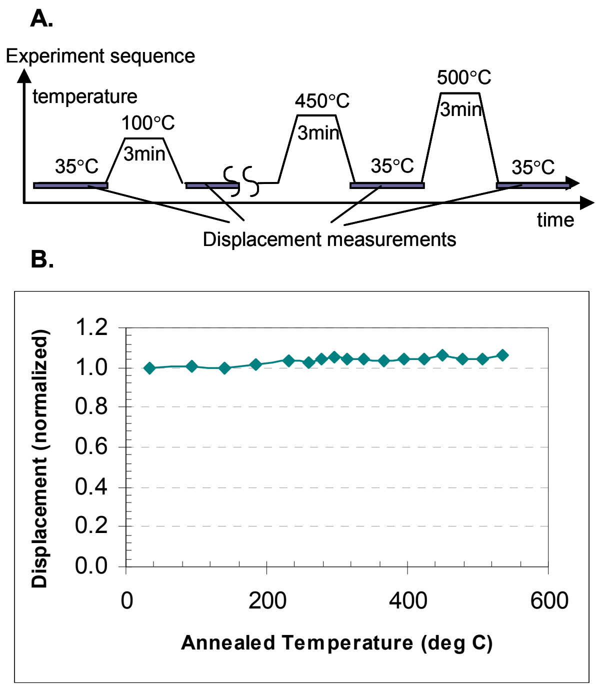

Figure 9: Displacement measurements after each annealing cycle. (A) Experimental sequence, (B) measured displacement results as a function of annealing temperature.

One of the challenges many researchers face during PZT sputtering development is film reproduceability. As the deposition chamber is coated with insulating film with successive formation of films, the electric potential of the chamber wall begins to change which results in a poor film reproducibility. We have made necessary modifications in the deposition chamber to overcome this problem, and now have very reproduciable, high volume production capability (Fig. 10).

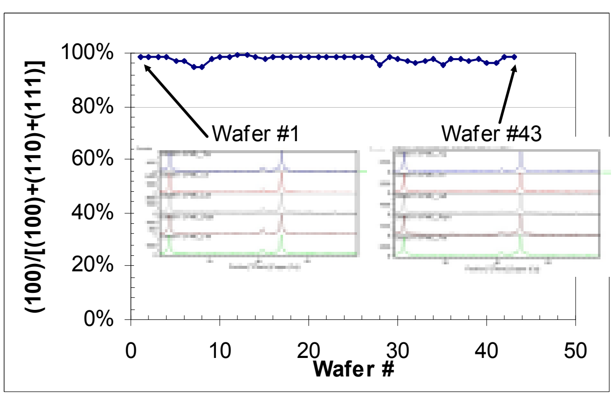

Figure 10: XRD history of successive film formations

7 CONCLUSION

Thus, we have developed a method of forming high performance PZT films on 6” wafer with good uniformity across a wafer and excellent repeatability. Our PZT film has an unusually high content of Nb dopant (13%) which results in ×1.7 higher piezoelectric coefficient than un-doped sputtered PZT films. The x-ray diffraction patterns of our PZT film demonstrate that film is in a perovskite phase with (100) orientation which partly accounts for its high piezoelectric performance. The polarization axes have been already aligned as deposited, making a post-deposition polarization process unnecessary. A displacement measurement using a diaphragm structure yielded d_{31}= -250pm/V. High piezoelectric constant of the film was confirmed by a 4-point cantilever bending experiment by outside vendor (aixACCT) which yielded $e_{31,f}$= - 23.1 C/m^2.

These unique and superior features of the sputtered PNZT film will create new opportunities in the MEMS field. The high piezoelectric coefficient of the film enables us to shrink device sizes down while keeping the same level of displacement. This will not only lower the production cost, but also enables us to build new high density array devices. Its durability against high temperature will enable us to easily integrate the material with high temperature post processes, such as CVD film deposition, high temperature wafer bonding, and solder reflow processes. Such a piezoelectric film with a high piezoelectric coefficient and durability will open up a new spectrum of MEMS applications.

REFERENCES

[1] P. Muralt, J. Micromech. Microeng., 10, 136, 2000.
[2] R.A. Wolf, S. Trolier-McKinstry, J. Appl. Phys., 95, 1397, 2004.
[3] N. Ledermann, P. Muralt, J. Baborowski, M. Forester, J.P. Pellaux, J. Micromech. Microeng., 14, 1650, 2004.
[4] Y. Sakashita, T. Ono, H. Segawa, K. Tominaga, M. Okada, J. Appl. Phys., 69, 8352, 1991.
[5] M. Shimizu, H. Fujisawa, T. Shiozaki, J. Cryst. Growth, 174, 464, 1997.
[6] R. Takayama, Y. Tomita, J. Appl. Phys., 65, 1666, 1989.
[7] I. Kanno, H. Kotera, K. Wasa, T. Matsunaga, T. Kamada, R. Takayama, J. Appl. Phys., 93, 4091, 2003
[8] M. Lebedev, J. Akedo, Japan. J. Appl. Phys., 41, 6669, 2002.
[9] E. Fujii, R. Takayama, K. Nomura, A. Murata, T. Hasegawa, A. Tomozawa, S. Fujii, T. Kamada, H. Torii, IEEE Trans. Ultrason., Ferroelectr., Freq. Control, 54, 2431, 2007.
[10] T. Fujii, Y. Hishinuma, T. Mita, and T. Arakawa, Solid State Commun.., 149, 1799, 2009.
[11] T. Fujii, Y. Hishinuma, T. Mita, T. Naono, Sens. Actuators, A, 163, 220, 2010.
[12] M. Yokosuka, T. Ochiai, M. Marutake, Japan J. Appl. Phys. 30, 2228, 1991.
[13] K. Prume, P. Muralt, F. Clame, T. Schmitz-Kempen, and S. Tiedke, J. Electroceram. 19, 407, 2007.

NSTI-Nanotech 2012, www.nsti.org, ISBN 978-1-4665-6275-2 Vol. 2, 2012